

Optical signal processing using electro-absorption modulators

J. Mørk, F. Romstad, S. Højfeldt, L. Oxenløwe,
K. Yvind, L. Xu, F. Öhman, L. J. Christiansen, A. Tersigni
Research Center COM, Technical University of Denmark
Build. 345v, DK-2800 Kgs. Lyngby, Denmark. E-mail: jm@com.dtu.dk

K. Hoppe, M. Løbel and J. Hanberg
GiGA Aps – an Intel Company, Mileparken 22, DK-2740, Skovlunde, Denmark

Reverse-biased semiconductor waveguides are efficient saturable absorbers and have a number of promising all-optical signal processing applications. Results on ultrafast modulator dynamics as well as demonstrations and investigations of wavelength conversion and regeneration are presented.

Keywords: Electro-absorption, modulator, optical processing, ultrafast dynamics

Introduction

Primary incentives for the use of all-optical signal processing in optical communication system are the larger data rates and increased flexibility that all-optical devices offer, as well as the cost-reduction that may be achieved by avoiding conversion back and forth between the optical and the electronic domain. To be practical and competitive, all-optical switching devices should fulfill criteria similar to those of electronic devices: They should be small and allow for integration of different functionalities, and have the potential for cheap mass-production.

Presently, various kinds of devices comprising a semiconductor optical amplifier (SOA) as the main active element are among the primary contenders for integrated all-optical devices [1]. The large values of gain and differential gain that may be achieved in SOAs allow switching with power levels in the range of milliwatts, and various functionalities have been demonstrated using a number of different schemes at speeds in excess of 100 Gb/s [2]. Electro-absorption modulators (EAMs), i.e., p-i-n waveguide structures quite similar to SOAs, but reverse biased, have been developed with the main purpose of electrically modulating an injected CW optical signal at high data rates and with low chirp. Presently, high-quality EAMs are available at bitrates up to 40 Gb/s. However, it has been demonstrated that the EAM has a number of other interesting applications, both when modulated electrically but also under optical control [3,4]. The optical control of an EAM, which is the main focus of this paper, relies on cross-absorption modulation between two optical beams in the device, quite similar to the effect of cross-gain modulation at play in SOAs. A major difference from an SOA is the fact that in an EAM the recovery time is governed mainly by carrier sweep-out from the active region under an applied external (reverse) field, which may lead to recovery times in the picosecond region. On the other hand, being an absorptive device, an optically controlled EA needs to be pumped by a strong optical beam in order to exhibit a strong modulation contrast.

Applications of electro-absorption modulators

Figs. 1 and 2 show examples of various EA applications, where the device is modulated either electrically (Fig. 1) or optically (Fig. 2). When a reverse bias is applied to a quantum-well (QW) EAM, the absorption of the device changes due to the quantum-confined Stark effect. This effect forms the basis of the so far most common application of EAMs; the imprinting of data onto a CW signal generated by a laser (external to the EAM or monolithically integrated with it). A main advantage of this configuration is the lower chirp compared to a directly modulated laser. This

application is illustrated in Fig. 1a, along with an example of a 40 Gb/s eye diagram for a ridge waveguide quantum-well (QW) type modulator operating at 1550 nm.

Fig. 3 shows examples of measured and calculated absorption spectra at different reverse voltages. There is always a trade-off between obtaining a low insertion loss in the on-state (the transmissive state) and getting a low modulation amplitude (that is, the voltage modulation span required to obtain a certain, say 10 dB, extinction ratio of the modulated optical signal). In the electrical demultiplexing application, one utilizes the nonlinearity of the transmission versus voltage characteristic of the EAM to open a switching window in the EAM transmission that may be significantly narrower than the applied electrical signal would seem to imply. Also, the possibility of electrically generating a short switching (transmission) window in the EAM may be used for recovery of the base-rate clock signal for a high-data rate optical-time-division-multiplexed (OTDM) signal; e.g. the recovery of the 40 GHz clock signal from a 4×40 Gb/s signal. In this case, the EAM will usually be part of a phase-locked loop incorporating a voltage-controlled oscillator. As an example of the versatility of an EAM, it may be mentioned that it has been shown to work as the only active component in the transmitter and the receiver in an entire system operating at 160 Gb/s [5], or even at 320 Gb/s when using polarization multiplexing [6].

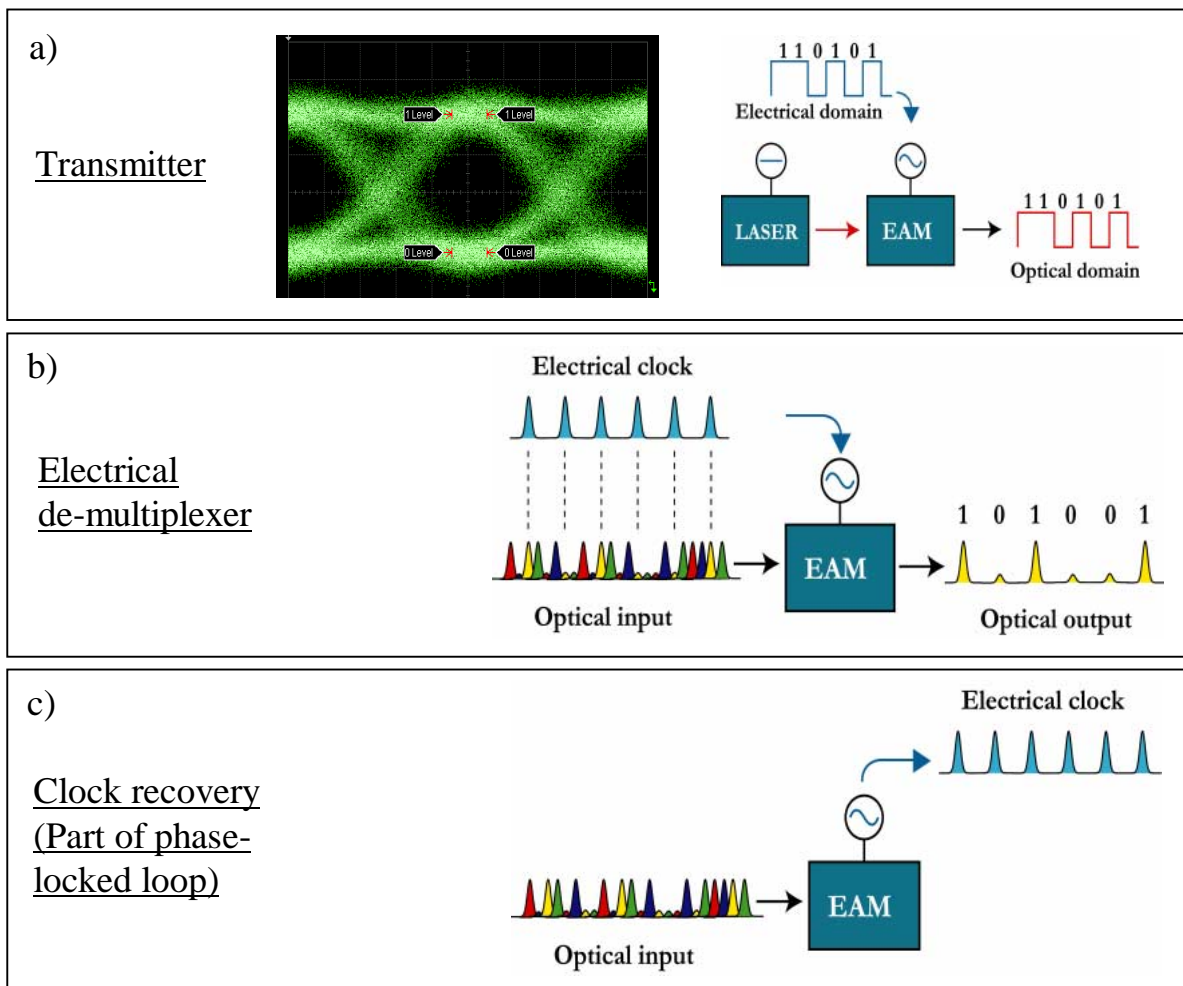


Fig. 1 Applications where the EAM is electrically controlled. a) Standard transmitter application. b) Electrical de-multiplexing may be achieved by utilizing the nonlinear transmission characteristic of the EAM. c) In (subharmonic) clock recovery one utilizes the EAM as a nonlinear mixer between an electrical clock signal and the data signal.

As mentioned, the optical control of an EAM relies on cross-absorption modulation between two optical beams in the device. A strong optical (pump) signal injected into the waveguide will thus reduce the material absorption, thereby increasing the transmission of another (probe) signal injected into the waveguide. The effects leading to absorption bleaching are bandfilling induced by the carriers excited by the pump signal, as well as the screening of the external field that these carriers induce, which in turn decreases the field-induced absorption. In contrast to the use of cross-gain modulation in an SOA, an EAM thus conserves the polarity of the signal; there is no data inversion. All-optical wavelength conversion, e.g., may be achieved in a manner much similar to the case of SOAs, cf. Fig. 2c. Presently all-optical wavelength conversion has been achieved at data rates of 40 Gb/s [3,4,7].

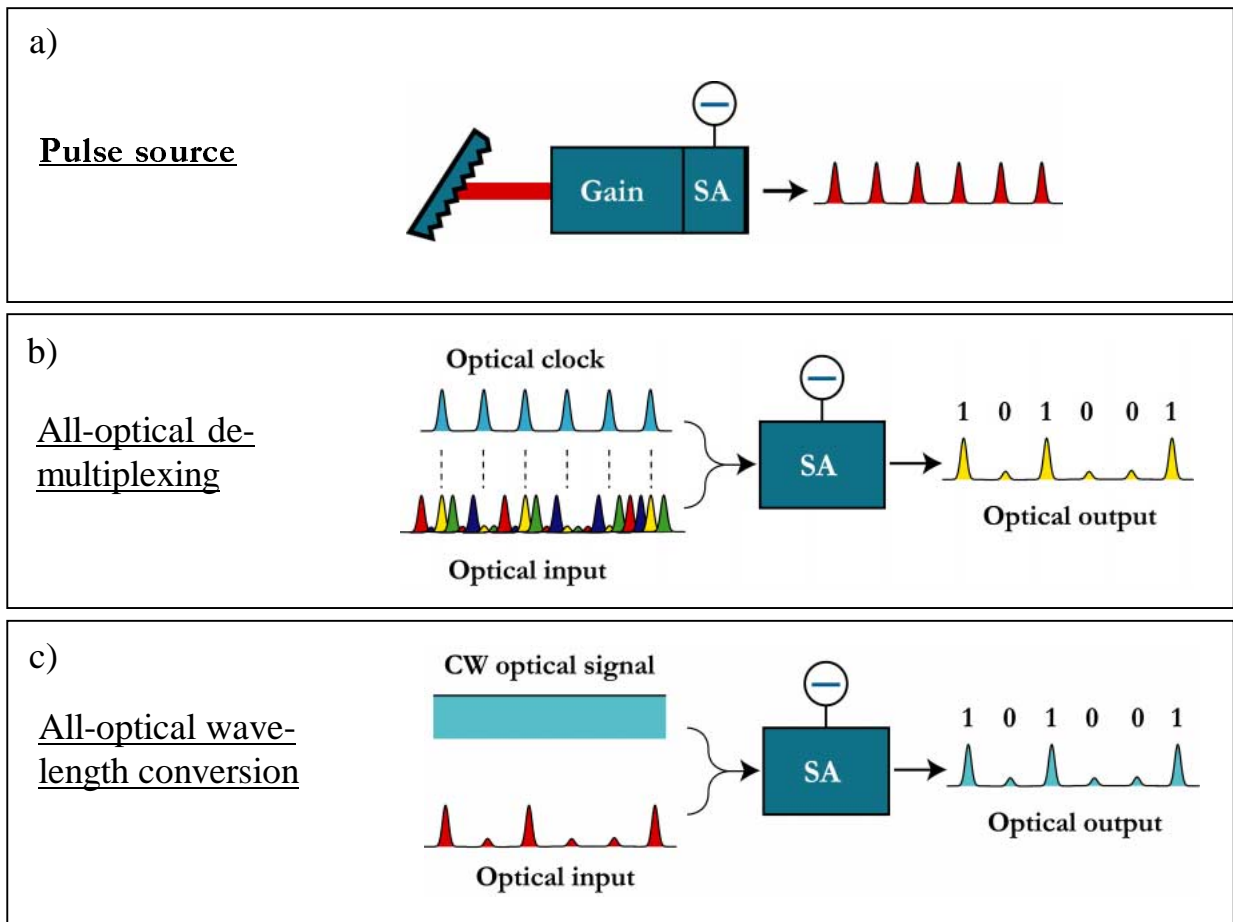


Fig. 2 Applications where the EAM is optically controlled. a) Saturable absorber (SA) element in mode-locked semiconductor laser. b) All-optical demultiplexing, where a strong optical clock signal, through band-filling and screening, opens up a narrow switching window for an optical data signal. c) All-optical wavelength conversion, where the data signal is imprinted on a (weak) CW data signal at another wavelength.

Basic properties of electro-absorption modulators

In Fig. 3 we compare measured and calculated absorption spectra (TE polarized light) for a 10 QW ridge waveguide structure. The qualitative agreement is quite good; the reason for the lower measured absorption is believed due to residual waveguide transmission, not accounted for by the model. The model for the absorption consists of a self-consistent solution of Schrödinger's equation for the wavefunctions of the quantum wells and Poisson's equation for the field and charge distribution across the heterostructure [8]. The bandstructure of the semiconductor is treated quite simplistically through parabolic subbands.

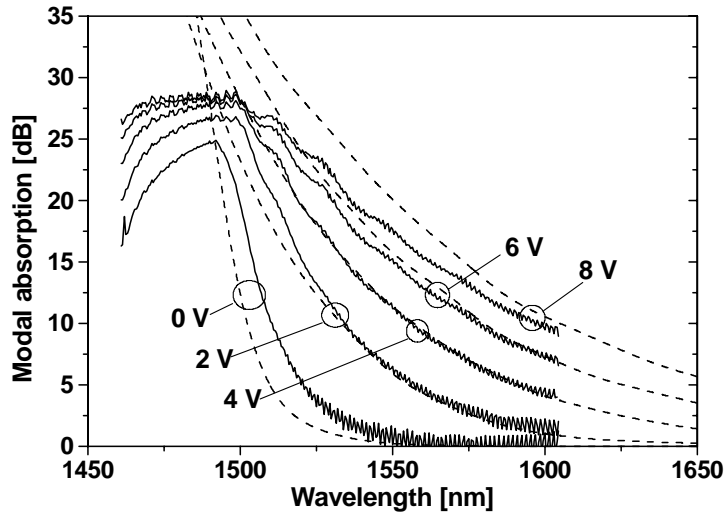


Fig. 3 Measured and calculated absorption spectra for a 250 μm long, 10 QW ridge waveguide structure for different values of reverse voltage. An insertion loss of 10 dB has been subtracted from the experimental curves.

Under electrical modulation, a most important device characteristic limiting the modulation bandwidth is the intrinsic device capacitance. Travelling wave configurations have been adopted in order to improve the bandwidth [9], and may extend the bandwidth beyond 40 Gb/s, which can be reached using standard electrode designs. In the case of optical modulation, however, a significant amount of carriers are generated in the QWs, and a number of transport processes, illustrated in Fig. 4, determine the speed of the device.

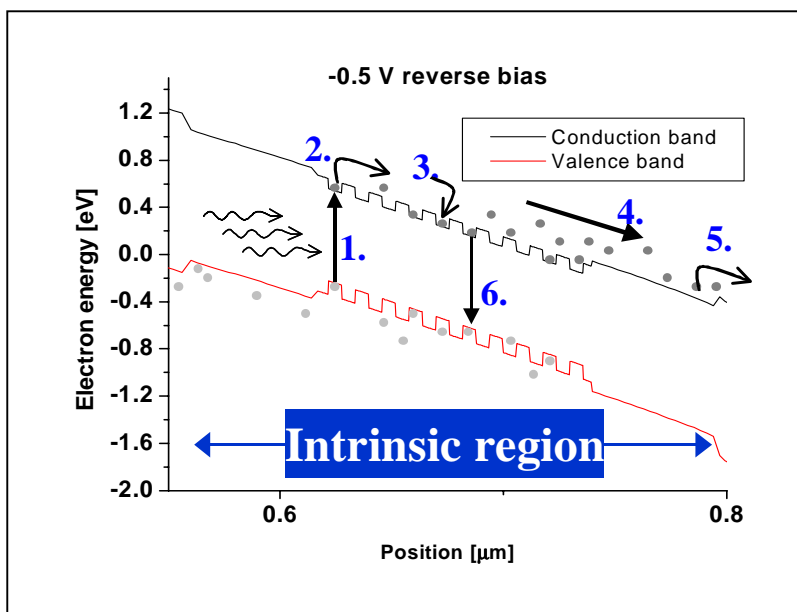


Fig. 4 Schematic illustration of transport processes in the intrinsic region of an EAM. (1) Carrier excitation by absorption of a photon. (2) Carrier escape from QWs. (3) Carrier recapture. (4) Drift-diffusion transport. (5) Transport over hetero-junctions. (6) Recombination.

The speed of the EAM under optical excitation can be measured using a pump-probe technique employing short optical pulses. In our case we use a heterodyne detection technique [10], which allows simultaneous measurement of the temporal change of the absorption as well as the refractive index following excitation by a short optical pulse. Fig. 5a shows the measured probe transmission for an EAM with a reverse bias of 10 V when a 200 fsec pump pulse with an energy of 3 pJ excites the EAM at time zero. The transmission is normalised to 1 prior to the excitation. The probe transmission has two main components: A fast component, with a characteristic relaxation time on the order of a couple of picoseconds, and a slow component with smaller amplitude, which relaxes on a time scale of the order of 100 ps. The measurements are seen to be well fitted by a double exponential fit, leading to values for the amplitude of the two components and their characteristic (1/e) relaxation times. Pump-probe measurements have been carried out for a number of different reverse voltages, and in Figs. 5b and c we show the corresponding variation of the time constants and the amplitudes. It is observed that at low reverse bias the two components have similar time constants, but as the voltage is increased, one of these become much faster and dominant in amplitude. Although the slow component seems relatively small at reverse voltages exceeding, say, 4V, it has to be kept in mind that for high data rate applications one may get an accumulated build up of carriers in the device. Single pulse pump-probe measurements are thus not sufficient to conclude on the actual system application of the device.

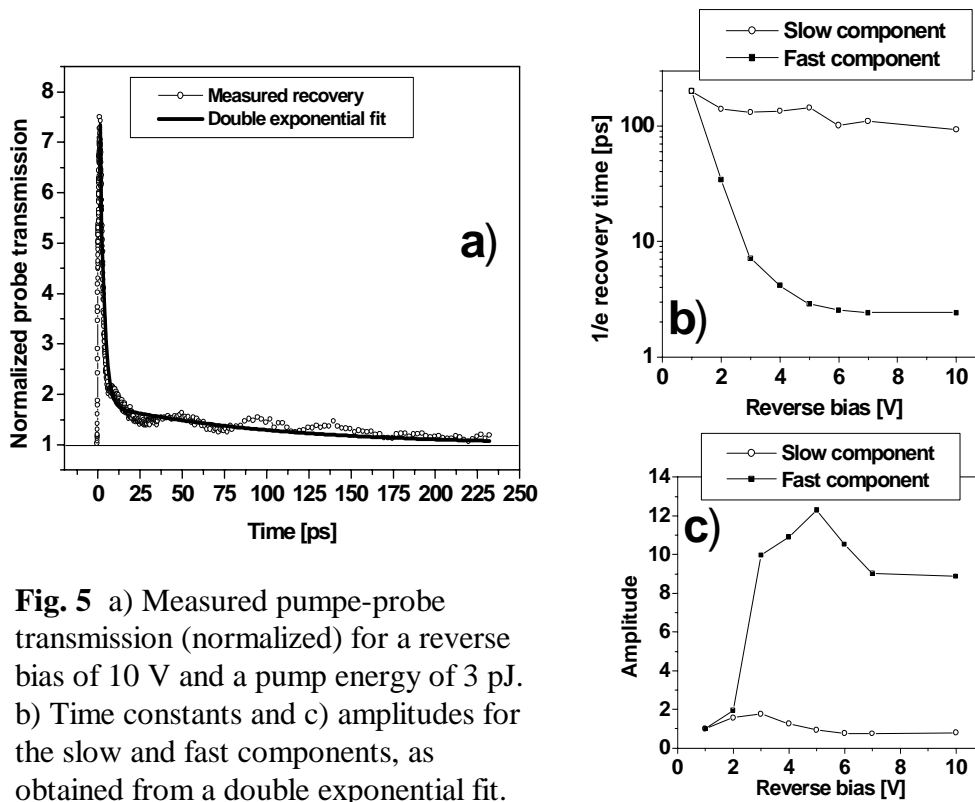


Fig. 5 a) Measured pump-probe transmission (normalized) for a reverse bias of 10 V and a pump energy of 3 pJ. b) Time constants and c) amplitudes for the slow and fast components, as obtained from a double exponential fit.

The association of the different time constants with the physical transport processes in the QW structure is not obvious. The fast component may well reflect carrier escape from the quantum wells due to thermionic emission or tunnelling (process (2) in Fig. 4), see e.g. [11], whereas the slower component could be due to screening of the electrical field, induced by carriers trapped at the

heterojunction interfaces (process (5) in Fig. 4), cf. [12]. Support for this interpretation is found from Fig. 6, which shows examples of calculated probe transmission curves based on our dynamical model for the EAM, including the carrier and electric field dynamics of the device. In agreement with [12] it is found that carrier pile-up at the edges of the heterostructure may significantly slow the overall recovery through a prolonged influence of field screening. Results are shown in Fig. 6d for two different separate confinement structures, i.e., a one- and a two-step structure. In the two-step structure, the rate of thermionic emission is significantly enhanced. Also, the calculations in Fig. 6b illustrate a strong influence from the process of recapture into QWs. Thus, if the recapture time is small, the carriers are transported, rather than by uniform drift in a strong electrical field, by a “hopping” motion from well-to-well, leading to a increase of the relaxation time of the slow component in the recovery. This could explain the experimental observation of a long recovery tail.

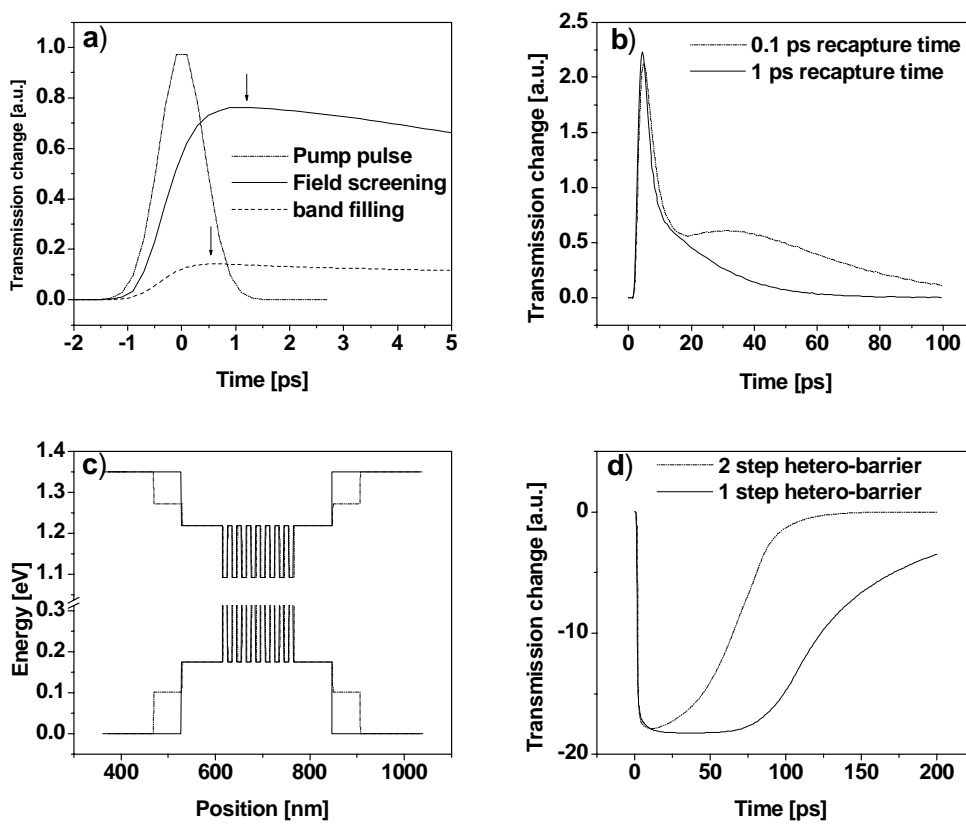


Fig. 6 Simulation results for an MQW EAM. a) Bandfilling and field screening contributions to the absorption dynamics following excitation by a 1 ps wide pulse with energy 1 pJ. b) The effect of recapture in an 8 QW structure. c) Banddiagrams for two different separate confinement structures, i.e., with one or two steps. d) Absorption changes induced by field screening for the two structures.

We have also found that for strong pump pulse energies the recovery may be significantly slowed down. The observation is well accounted for by the dynamical model, and is explained by an initial very strong field screening due to many carriers excited into the separate confinement region. Until a certain fraction of these carriers have recombined, the field cannot build up and the recovery proceeds very slowly with characteristic time similar to the carrier lifetime. However, once the field gains strength the recovery is accelerated and characterized by the sweep-out time from the separate confinement region.

Wavelength conversion

We now briefly present some examples of wavelength conversion in EAMs and the dependence on parameters such as reverse bias and pump power [7,13]. The experimental set-up is shown in Fig. 7. An erbium fibre ring laser (EFRL), working at 1552nm, generates short optical pulses at 10GHz which are data modulated by a MZ modulator and then optically multiplexed to 40Gb/s, to be used as the pump signal. The probe light, generated by a tunable laser (TL), is injected into the EAM together with the pump signal, and through the process of cross-absorption modulation the pump data signal is transferred to the probe. The converted signal is afterwards demultiplexed back to 10Gb/s by a non-linear optical loop mirror (NOLM) which consists of 500m highly non-linear dispersion-shifted fibre (HN-DSF).

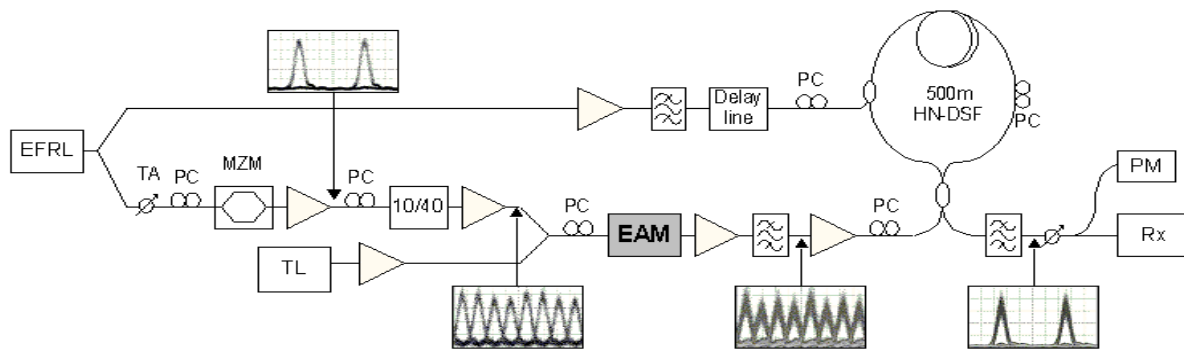


Fig 7. Experimental set-up. EFRL: Erbium fibre ring laser, TA: Tunable laser, PC: Polarization control, TL: Tunable laser

In Fig. 7 the eye diagram of the original signal at 1552nm and that of the converted signal at 1561nm are depicted, together with the signal demultiplexed by the NOLM. In this case the receiver sensitivity for a Bit-Error-Rate (BER) of 10^{-9} is about -26.6dBm , which can be further improved by optimising the receiver and the NOLM.

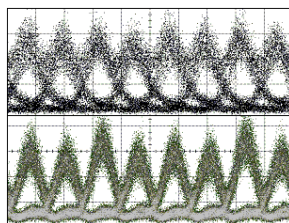


Fig 8. The converted signal for pump power levels of 16dBm (upper) and 20dBm (lower).

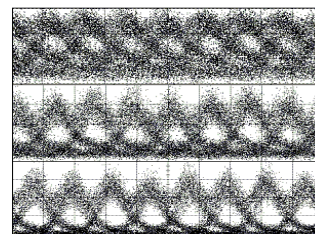


Fig 9. The converted signal for 16dBm pump power @ reverse bias of -1.5 V (upper), -2.0 V (middle) and -2.5 V (lower).

In Fig. 8 we compare two cases corresponding to pump power levels of 16 dBm and 20 dBm, showing that higher pump power leads to a better eye-opening. The BER quoted above was thus obtained for 20dBm pump power, while it wasn't possible to achieve such a low BER at a pump power level of 16dBm. The dependence of bias voltage of the EAM was also studied. As shown in Fig. 9, under a fixed pump power (16dBm), higher reverse bias is beneficial. Lower bias thus leads to a long "tail" in the eye diagram, which is attributed to a longer carrier recovery time under weak electric field.

It should be noted that although the present results indicate higher pump power to be beneficial, one should be careful in the use of excessive pump power levels. Since the number of photo-generated carriers increases with pump power, the recovery time may suddenly be drastically increased, as mentioned earlier, due to excessive field screening preventing carrier sweep-out. This may be counterbalanced by the use of a higher reverse bias, which will, however, also increase the insertion loss of the device. Beyond this, the reliability of an EAM under such extreme conditions also needs consideration.

The performance at various probe wavelengths has also been investigated and it is found that the original signal at 1552 nm can be converted to wavelengths ranging from 1537 nm to 1564 nm, resulting in clear and open eyes. This suggests that EAM-based wavelength conversion has a wide wavelength range of operation. It is, however, found that in some wavelength ranges an appreciable dc-offset exists, which limits the achievable extinction ratio. The dc component reflects the fact that a part of the probe beam passes through the device without being modulated. Measurements of the chirp properties of EAM-wavelength converted signals have shown that shorter wavelength operation lead to lower chirp (α -) parameter. In all cases investigated, the output chirp was lower than the input chirp, suggesting the capability of an EAM-based wavelength converter to reduce chirp and even possibly generate a negatively chirped signal.

Regeneration and integrated devices

The regenerative properties of a saturable absorber due to absorption bleaching are well documented, both as a stand-alone component [14,15] and integrated with a semiconductor optical amplifier (SOA) [16,17]. The signal improvement is achieved by suppressing low intensity noise on the zero-level while the high intensity one-level bleaches the absorption and thus experience much less absorption. We have recently proposed [18] a novel device, which contains a cascade of SOAs and electro absorbers (EA); see Fig. 10. We have in mind a monolithically integrated device, with forward and reverse biased waveguide sections. This is similar to a mode-locked laser design, and the device performs signal shaping and pedestal suppression similar to the shaping of pulses circulating in a mode-locked laser. We have theoretically analyzed the regenerative properties and noise of the proposed device.

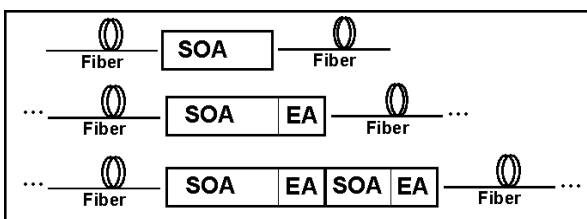
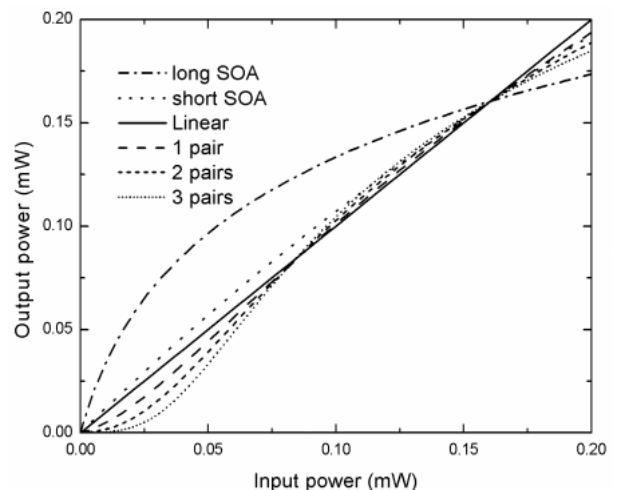


Fig. 10 Investigated devices, containing a cascade of SOA and EA sections (above). Transfer function, i.e., output power versus input power for different device combinations (to the right).



The static transfer functions for different combinations of single SOAs and SOA-EA pairs are shown in Fig. 10. The transfer functions include the fibre loss, which has been chosen to precisely compensate the device gain at the power level for the logical "1", i.e. at about 0.16 mW where the output power from one span is equal to the input power. The total gain of the modules at this operating point is 18.6 dB for the long SOA and 10.3 dB for the SOA-EA pairs, the short SOA and the linear amplifier. The non-linear transfer functions result from the saturation of the EA absorption and the SOA gain. The small signal absorption of the EAs is high and suppresses the low intensity noise, but the device is bleached at higher powers, if the saturation power of the SOA is high enough. At even higher powers the SOA saturates and gives a flat transfer function that redistribute the noise at the "1"-level. Since the device operates in saturation the response time needs to be fast compared to the bit rate; justifying a quasi-cw approach for evaluating the BER-penalties from amplified spontaneous emission noise [19]. The analysis also has to include the fact, that insertion of an absorptive element needs to be balanced by an increase of the SOA gain, thus increasing the amount of amplified spontaneous emission (ASE) noise. The resulting BER is plotted in Fig. 11 versus the total link loss for one, two and three SOA-EA pairs as well as for the long and short SOA and for the linear amplifier with no noise redistribution. For few regenerators the noise of the input signal dominates, but as more ASE accumulates from several regenerators, the BER increases from the added noise. For many regenerators the BER strongly increases for the case of stand-alone SOAs, while the incorporation of saturable absorbers is seen to slow down the BER accumulation. In particular it is seen that for a large number of regenerators the sharper transfer functions of the multi-section devices do indeed improve the performance of the system.

The analysis thus suggests that substantial improvements in the cascadability of fibre-amplifier links can be obtained by incorporating saturable absorber sections, i.e. the device has regenerative properties.

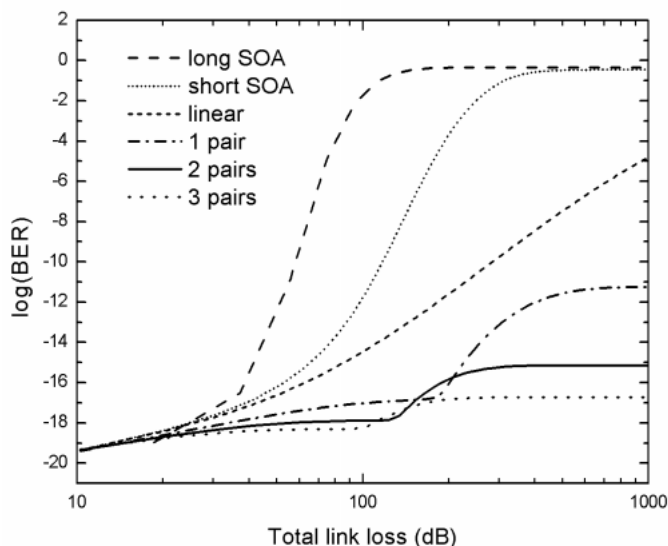


Fig. 11 Calculated BER versus total link loss for concatenated spans of fibers and regenerators. Different device configurations are compared

Summary and conclusions

Electro-absorption modulators offer a number of interesting opportunities for performing all-optical signal processing at high bitrates. Wavelength conversion, de-multiplexing, regeneration, and other more advanced functionalities, such as label swapping, have been demonstrated using relatively simple device geometries. One of the main advantages of the electro-absorption modulator in

comparison to other all-optical switching devices, e.g. interferometers employing semiconductor optical amplifiers, is the simple device geometry and its simple operation. On the other hand, electro-absorption modulators require quite high optical pump power and the device design needs to ensure that a fast sweep-out of carriers can be sustained at these high pump power levels. An example of a new type of regenerator exploiting the linear and nonlinear properties of electro-absorption modulators as well as semiconductor optical amplifiers was presented. Such integrated designs may offer new and improved functionalities in the future.

References

- [1] K. Stubkjaer, *IEEE J. Select. Topics Quantum Electron.*, vol. 6, pp. 1428-1435, Nov. 2000.
- [2] S. Nakamura, Y. Ueno and K. Tajima, *IEEE Photon. Technol. Lett.*, vol. 13, pp. 1091-1093, Oct. 2001.
- [3] N. Edagawa, *IEICE trans. on electronics*, vol. E81-C, No. 8, pp. 1251-2157, 1998.
- [4] T. Otani et al., *J. Lightwave Technol.*, vol. 20, pp. 195-200, 2002.
- [5] B. Mikkelsen et al., *Proc. ECOC 2000*, paper 6.1.1, Munich, Germany, Sept. 2000.
- [6] B. Mikkelsen et al., *IEEE Photon. Technol. Lett.*, vol. 12, pp. 1400-1402, 2000.
- [7] L. Xu et al., *Proc. IEEE/LEOS Annual Meeting*, pp. 111-112, Glasgow, Nov. 2002.
- [8] S. Højfeldt et al., *IEEE J. Select. Topics Quantum Electron.*, vol. 8, pp. 1265-1276, 2002.
- [9] S. Irmscher et al., *Proc. ECOC 2002*, Paper 10.5.5, Copenhagen, Sept. 2002.
- [10] P. Borri et al., *Opt. Commun.*, vol. 169, pp. 317-324, Sep. 1999.
- [11] L. R. Brovelli et al., *J. Appl. Phys.*, vol. 76, pp. 7713-7719, Dec. 1994.
- [12] T. Yoshida et al., *Opt. Quantum Electron.*, vol. 33, pp. 735-743, 2001.
- [13] L. Xu et al., *ECOC 2002*, paper P1.26 (2002).
- [14] H. Yokoyama et al., *Tech. Dig. CLEO'98*, pp. 502-503, 1998.
- [15] S. Højfeldt et al., *J. Lightwave technol.*, vol. 18, 1121, 2000.
- [16] C. Knöll et al., *Opt. Commun.*, vol. 187 (2001), 141-153.
- [17] Z. Bakonyi et al. *IEEE Photon. Technol. Lett.*, vol. 12, pp. 570-572, 2000.
- [18] F. Öhman et al., *2002 IEEE/LEOS Annual Meeting Conference Proceedings*, pp. 895-896, Glasgow, Scotland, Nov. 2002.
- [19] P. Öhlén et al., *IEEE Photon. Technol. Lett.*, vol. 9, pp. 1011-1013, 1997.